

Evaluation of a Noise Reduction Procedure for Chest Radiography

Ryohei Fukui,* Rie Ishii,* Kazuhiko Kodani,* Yoshiko Kanasaki,† Hisashi Suyama,‡ Masanari Watanabe,§ Masaki Nakamoto§ and Yasushi Fukuoka§

*Division of Clinical Radiology, Tottori University Hospital, Yonago 683-8504, Japan, †Division of Radiology, Matsue City Hospital, Matsue 690-8509, Japan, ‡Division of Internal Medicine, Tottori Central Prefectural Hospital, Tottori 680-0901, Japan and §Division of Medical Oncology and Molecular Respiriology, Tottori University Hospital, Yonago 683-8504, Japan

ABSTRACT

Background The aim of this study was to evaluate the usefulness of noise reduction procedure (NRP), a function in the new image processing for chest radiography.

Methods A CXDI-50G Portable Digital Radiography System (Canon) was used for X-ray detection. Image noise was analyzed with a noise power spectrum (NPS) and a burger phantom was used for evaluation of density resolution. The usefulness of NRP was evaluated by chest phantom images and clinical chest radiography. We employed the Bureau of Radiological Health Method for scoring chest images while carrying out our observations.

Results NPS through the use of NRP was improved compared with conventional image processing (CIP). The results in image quality showed high-density resolution through the use of NRP, so that chest radiography examination can be performed with a low dose of radiation. Scores were significantly higher than for CIP.

Conclusion In this study, use of NRP led to a high evaluation in these so we are able to confirm the usefulness of NRP for clinical chest radiography.

Key words chest radiography; image processing; noise power spectrum; noise reduction procedure; observation

For digital radiography, the conventional film-screen system for X-ray radiography is replaced with computed radiography and a flat panel detector (FPD). In analog radiography, film density and changes in contrast depend on the exposure conditions, whereas in digital radiography, the X-ray image is dependent on the image processing that incorporates various parameters. The image processing procedure changes the exposure conditions for the X-ray device. Suitable radiograms can be achieved with digital radiography even by an inexperienced radiological technologist.

Digital X-ray image quality is adjusted based on 3 factors: contrast, sharpness and graininess. Optimization of image quality is affected by these 3 closely related factors. The graininess on an X-ray image is statistical noise

caused by the characteristics of the X-ray detector and variations in radiation doses. Reducing the radiation dose for patients is important, and the graininess in digital imaging is most affected by dose reduction. Therefore, the improvement of graininess can actually lead to reducing radiation doses.¹ There are many reports on image processing of the X-ray imaging,^{2, 3, 4, 5, 6} but excessive image processing can deteriorate image quality.^{7, 8}

The noise reduction procedure (NRP) is a function of the image processing software MLT-S (Canon Lifecare Solutions, Osaka, Japan). NRP analyzes the image noise superimposed on each spatial frequency component, and reduces noise by subtracting the noise from each spatial frequency component. Our aim in this study was to verify the usefulness of NRP in chest radiography compared with the current image processing. We performed 2 types of evaluations in the present study, a physical characteristic analysis of graininess, and observation. However, the 2 types of evaluations may not be correlated. Therefore, to optimize the image processing procedure conditions for chest radiography, we performed an overall evaluation of chest radiography using a phantom and various clinical cases during observation.

SUBJECTS AND METHODS

X-ray devices and phantoms

A DHF-1510S (Hitachi Medical, Tokyo, Japan) was used for X-ray equipment, and a CXDI-50G (Canon) was used as the X-ray detector. This detector is a terbium doped gadolinium oxysulfide (Gd₂O₂S:Tb) FPD employing indirect conversion with a pixel pitch of 0.15 mm. A burger phantom was used to evaluate density resolution, and a PBU-SS-2 chest phantom (Kyoto Kagaku, Kyoto, Japan), which simulates the chest structure, to simulate

Corresponding author: Ryohei Fukui

rfukui@med.tottori-u.ac.jp

Received 2013 September 24

Accepted 2013 November 5

Abbreviations: BMI, body mass index; BRH, Bureau of Radiological Health; C-D, contrast-detail; CIP, conventional image processing; FPD, flat panel detector; IQF, image quality figure; NIP, new image processing; NPS, noise power spectrum; NRP, noise reduction procedure

chest radiography. Both phantoms were used for observation. A high-resolution monitor ME355i2 (TOTOKU, Tokyo, Japan) was also used for observation. Images were analyzed using ImageJ image processing (NIH, Bethesda, MD).

Image processing for evaluation

An X-ray image processed by the current method is referred to as “conventional image processing (CIP)” in the present study. CIP is used in our hospital for chest radiography. An X-ray image processed by MLT-S is referred to as “new image processing (NIP)”. The noise reduction factor in NRP can be changed from 1 to 10 during radiography image processing. NRP with the associated noise reduction factor is referred to as NIP (factor 1) to NIP (factor 10), in the order of increasing image processing strength.

NRP is able to reduce image noise that is strengthened during image processing. Although image processing strengthens the noise, the radical nature of an image will reduce because of the method of noise reduction with NRP. Detection of a small signal is reportedly reduced by excessive processing.⁷ Therefore, in this study, we employed NIP (factor 5) and NIP (factor 7) for moderately and slightly strong image processing, respectively. Other processing conditions, for example, contrast and edge enhancement, were selected based on manufacturers’ recommendations.

Ethical considerations

The Ethics Committee of Tottori University approved the use of clinical images for the experiment (approval number 1143). We explained the study to the patients, and only the images provided were used for this study after obtaining consent from them.

Measuring the NPS

X-ray image noise was evaluated using the noise power spectrum (NPS). A decrease in the NPS value indicates an improvement in graininess. Images that emitted X-ray uniformly were used for NPS analysis. Only the image processing on the FPD console was changed for each acquired image, and these images were used for subsequent NPS analysis after output in formats used for digital imaging and medical communication. CIP and NIP (factor 5) were chosen for NPS analysis.

Evaluation of density resolution

The density resolution was evaluated by observation through the use of the burger phantom, which is a plate used to evaluate density resolution; the depth becomes gradually shallow laterally, and the diameter changes in

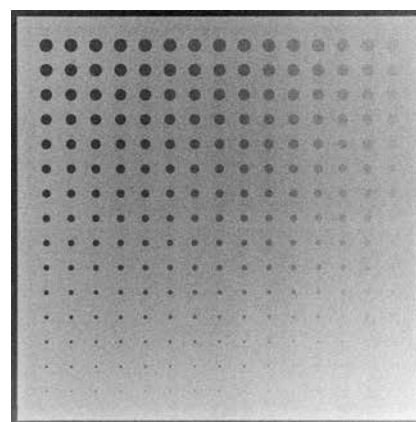


Fig. 1. Burger phantom X-ray image. The burger phantom is a plate used to evaluate density resolution; the depth becomes gradually shallow laterally, and the diameter changes in the lengthwise direction.

a lengthwise direction. The same geometric parameters were used with the burger phantom image for the clinical chest radiography. We placed an acrylic plate (20 cm) in front of the burger phantom to simulate the average thickness of a human body. Figure 1 shows the X-ray image of the burger phantom. The observers evaluated the limit of detection with this signal. CIP and NIP (factor 5) were used for this evaluation. Eleven radiological technologists (experience: 2–36 years) in our hospital participated in the observation. The density resolution was calculated from the results of the observation and expressed as a contrast-detail (C-D) diagram. The curve of the C-D diagram (below) shows high-density resolution. The image quality figure (IQF) was calculated from the same results.⁹ The IQF, obtained from n lines of the burger phantom, was calculated using the formula:

$$IQF = \sum_{i=1}^n C_i \times D_{i.min} \quad (1)$$

where C_i is the signal diameter of line i , and D_i is the signal thickness in line i detectable by an observer. D_i decreases as the density resolution increases. Thus, a small IQF denotes a high density resolution. To investigate the change in IQF according to exposure dose, we prepared the evaluation samples with NIP(factor 5) that were obtained at various exposure times. An exposure time of 25 ms is equivalent to an exposure dose of 100%: we employed exposure times of 20 ms (80%), 16 ms (64%) and 12 ms (48%).

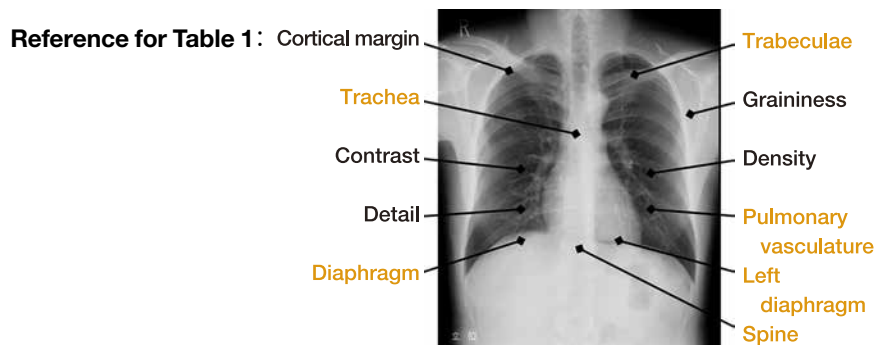
Evaluation using a chest phantom

The chest phantom simulates the chest structure for use in chest radiography. Radiograms of the chest phantom were acquired to compare image-processing methods

Table 1. Assessment items of the BRH method: (a) anatomic landmarks and (b) physical parameters

(a) Anatomic landmarks				
i	Bony thorax (ribs & clavicles) (clearness of the edge)	Cortical margins	a Optimally visualized	(5)
			b Adequately visualized	(4)
			c Poorly visualized	(2)
			d Not visualized	(0)
		Trabeculae	a Optimal detail	(5)
			b Adequate detail	(4)
			c Poor detail	(2)
			d Not visualized	(0)
ii	Retrocardiac area	Left diaphragm	a Totally visualized	(15)
			b Partially visualized	(7)
			c Not visualized	(0)
		Spine	a Too well visualized	(7)
			b Optimally visualized	(15)
		c Acceptably visualized	(7)	
		d Poorly visualized	(3)	
		e Not visualized	(0)	
iii	Diaphragm (diaphragm outline)	a Both visualized	(15)	
		b Right only	(7)	
		c Left only	(7)	
		d Not visualized	(0)	
iv	Trachea (visible to)	a Left main stem bronchus	(15)	
		b Carina	(10)	
		c Neck and upper mediastinum	(5)	
		d Not visible	(0)	
v	Pulmonary vasculature (maximum measurable to)	a Right costophrenic angle	(30)	
		b Right mid-lung	(20)	
		c Right descending pulmonary artery	(10)	
		d None	(0)	
(b) Physical parameters				
vi	Contrast	a Optimal	(35)	
		b Good	(23)	
		Poor, but diagnostic	c Too gray	(11)
			d Too black/white	(11)
		Unacceptable, not diagnostic	e Too gray	(0)
			f Too black/white	(0)
vii	Graininess	a No grain visible	(20)	
		b Minimal grain	(13)	
		c Grainy, but dose not interfere with diagnosis	(6)	
		d Grain interferes with diagnosis	(0)	
viii	Density	a Optimal	(15)	
		b Good	(10)	
		Poor, but diagnostic	c Too dark	(5)
			d Too light	(5)
		e Unacceptable	(0)	
iv	Detail	a Optimal	(30)	
		b Good	(20)	
		c Poor detail, but dose not interfere with diagnosis	(10)	
		d Lack of detail interferes with diagnosis	(0)	

() shows the score when the observer selected on the chest radiogram evaluation.



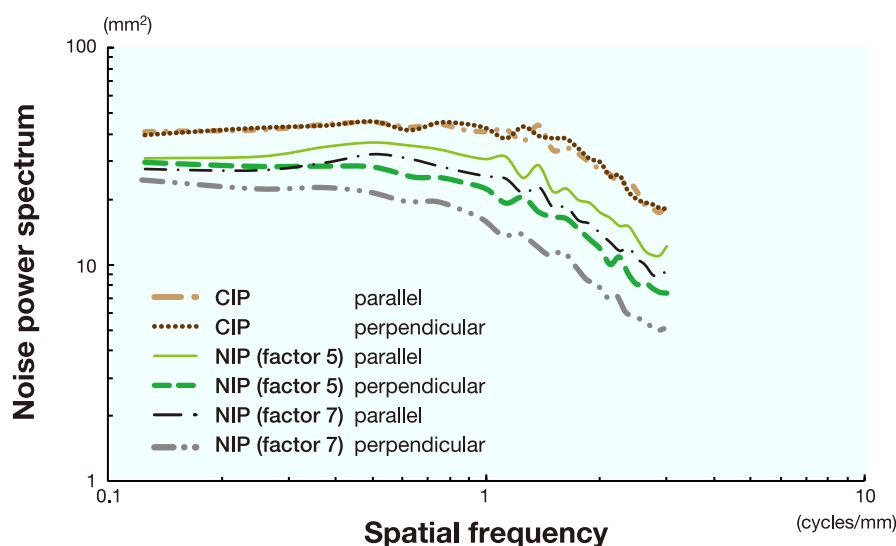


Fig. 2. Noise power spectrum (NPS). The characteristic for horizontal direction and vertical direction is referred to as “parallel” and “perpendicular”, respectively. The NPS with NIP (factor 5) was smaller than that CIP in all spatial frequencies. CIP, conventional image processing; NIP, new image processing.

CIP, NIP (factor 5) and NIP (factor 7). The geometry for the chest phantom radiography is similar to that for chest radiography of patients in our hospital. The observers for this experiment were the same observers in the burger phantom study. Observation was similar to that done for the clinical interpretation of radiograms (i.e. room lighting, high-resolution monitor, etc.). We employed the Bureau of Radiological Health (BRH) method for scoring the chest phantom images (Tables 1a and b).¹⁰ The BRH method is used for the overall evaluation of chest radiography using a screen or film. The chest radiography score was calculated as an anatomical index (perfect score: 100 points) and a physical index (perfect score: 100 points). We changed the grand total to an overall perfect score of 100 using the following formula:

$$\frac{\text{Total score of AI} + \text{total score of PI}}{200 - N} \times 100 \quad (2)$$

where AI is the anatomical index, N, the evaluation item and PI, the physical index. However, if the observer could not evaluate an image because of a lesion, we deducted the score for the N from the denominator. The Wilcoxon signed-rank test was used to test for statistical significance, with the significance level set at $P < 0.05$.

Evaluation using clinical chest radiography

Forty patients [28 men, 12 women, mean (*s*) age: 63.9 (16.0)] involved in diagnostic chest radiography in our hospital (examinations: February to April, 2009) were subjected to the observation experiment. Diagnoses included 5 normal subjects, 13 patients with lung cancer (including postoperative diagnosis), 13 patients with interstitial pneumonia, 3 patients with sarcoidosis, 2 patients with nontuberculous mycobacterial infection and 4 patients with other diseases. The geometry conditions

for X-ray radiography were as follows: upright position, posterior-anterior view, focus to detector distance of 200 cm. Four pulmonologists and 2 radiologists took part in this observation experiment. All observers were prepped using other samples of radiograms of the chest phantom beforehand and confirmed the evaluation region and criterion. CIP, NIP (factor 5) and NIP (factor 7) were used to process the chest radiograms, and the BRH method was used for scoring the images. All patients were classified and evaluated using the same methods. Classifications are described in the following section.

Subject classifications for chest radiography

All patients were classified according to body mass index (BMI), aeration of the lung and presence of a lung lesion, and evaluated with only 2 processing methods, CIP and NIP (factor 5).

Because graininess is most affected by variations in a patient’s physique, we classified all patients by BMI. A BMI less than 18.5 was classified as underweight; a BMI of 18.5 but less than 25, as normal and a BMI more than 25, as overweight.¹¹

Evaluations of chest radiograms are also affected by density variation in the lung field caused by aeration. The right diaphragm should be at the height of the posterior 10th rib under sufficient inhalation.¹² When the right diaphragm was positioned at the height of the 9th rib, the case was classified as “poor”. The case was classified as “good” when the right diaphragm was positioned at any height below the 9th rib.

To optimize image processing, it is important to evaluate chest radiograms with various lesions. We classified all patients with lung lesions into 4 patterns: interstitial markings, a nodule, a consolidation and a normal pattern.¹³

RESULTS

Figure 2 shows the NPS analysis results. An NPS with an NIP was smaller than that with CIP for all spatial frequencies. Moreover, the NPS was small when the image processing was strong.

Figure 3a shows the C-D diagram calculated in the burger phantom study. The curve for NIP (factor 5) was below that for CIP. Figure 3b shows the IQF value for each exposure dose. As shown in Fig. 3b, the IQF value with CIP was equal to the IQF value at 72% exposure dose with NIP (factor 5).

Table 2 shows the results of the observation with the chest phantom image. The total score for NIP (factor 7) was significantly higher than that for CIP. There was no difference in the total score between CIP and NIP (factor 5). Many assessment items for the BRH method with NIP were improved compared with CIP; in particular, the graininess score was significantly higher.

Table 2 also shows the results of observation with clinical chest radiography. The total scores of NIP (factor 5) and NIP (factor 7) were significantly higher than CIP ($P = 0.0002$, $P = 0.007$, respectively). The contrast and the graininess were improved compared with CIP. Because the evaluation of NIP (factor 5) was higher than that for NIP (factor 7), we estimated only CIP and NIP (factor 5) in the subsequent experiment in which all clinical cases were categorized.

Table 3 shows the results of observation with clinical cases categorized according to various conditions of the patients. For convenience, the CIP score is not included

in Table 3. For BMI, the scores of many assessment items for the BRH method were significantly higher than CIP. There was a tendency for the score to decrease as the BMI value increased; however, NIP (factor 5) reduced the magnitude of this decrease compared with CIP. For aeration of the lung, both the good group and

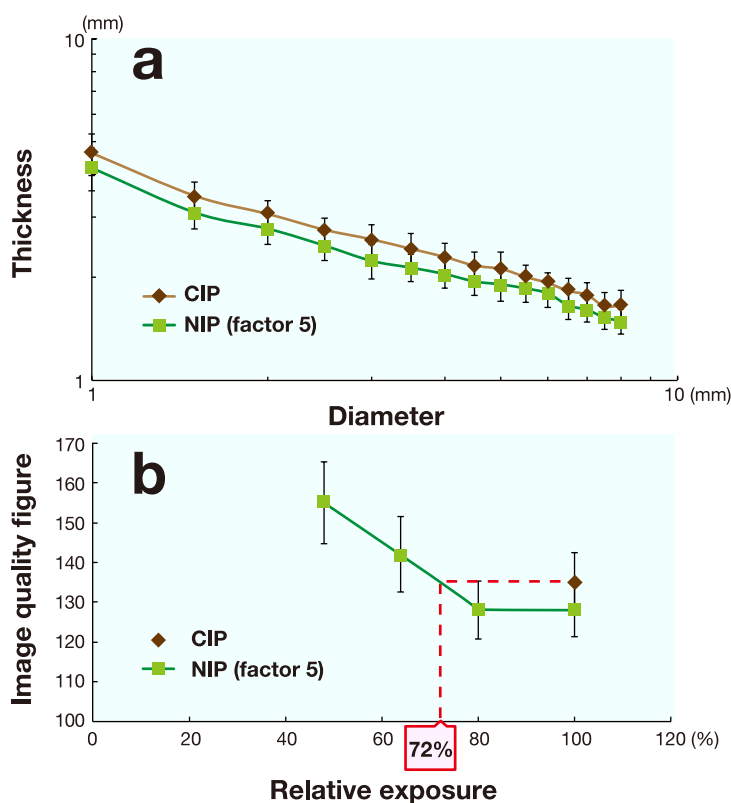


Fig. 3. The results of observation using the burger phantom.

a: Contrast-detail diagram.

b: Image quality figure.

CIP, conventional image processing; NIP, new image processing.

Table 2. The results of observation with the chest phantom and chest radiography

Assessment items	Chest phantom (mean [s])			Chest radiography (mean [s])		
	CIP	NIP (factor 5)	NIP (factor 7)	CIP	NIP (factor 5)	NIP (factor 7)
Cortical margins	3.67 [0.96]	4.22 [0.90]	4.22 [0.83]	4.09 [0.82]	4.27 [0.65]*	4.21 [0.65]*
Trabeculae	2.89 [1.0]	3.78 [1.1]	3.56 [1.2]	3.49 [1.3]	3.51 [1.4]	3.44 [1.3]
Left diaphragm	14.1 [3.5]	14.1 [2.2]	14.1 [2.2]	11.1 [5.5]	11.2 [5.4]	11.4 [5.3]
Spine	8.33 [5.0]	7.89 [4.6]	8.33 [4.5]	6.25 [4.7]	8.13 [4.8]*	8.04 [5.0]*
Trachea	10.7 [3.1]	10.4 [2.7]	10.4 [2.9]	13.1 [3.5]	13.5 [3.4]	13.4 [3.3]
Diaphragm	15.0 [0.0]	15.0 [0.0]	15.0 [0.0]	11.7 [5.5]	12.0 [5.2]	12.1 [5.2]
Pulmonary vasculature	25.6 [5.1]	23.7 [6.0]	25.6 [5.1]	20.1 [11]	20.9 [11]	20.8 [11]
Contrast	20.3 [6.7]	20.3 [6.7]	24.3 [4.5]	18.0 [8.9]	19.6 [9.2]*	19.0 [9.2]
Graininess	13.0 [4.9]	18.4 [3.1]*	18.4 [2.6]*	18.3 [3.0]	19.5 [1.8]*	19.5 [1.8]*
Density	8.89 [1.9]	8.89 [2.2]	8.89 [2.2]	9.26 [2.9]	10.2 [2.6]*	9.79 [2.6]*
Detail	21.1 [4.1]	21.1 [4.1]	21.1 [3.8]	18.4 [5.4]	19.3 [5.1]*	18.6 [5.0]
Total score	72.0 [21]	73.8 [19]	80.4 [15]*	70.0 [11]	74.0 [11]*	72.8 [11]*

CIP, conventional image processing; NIP, new image processing.

* $P < 0.05$: Comparison with the score of CIP.

Table 3. The results of observation with clinical cases categorized according to various conditions of the patients

	BMI (mean [s])			Aeration of the lung (mean [s])			Lung lesion (mean [s])		
	Under-weight	Normal range	Over-weight	Poor	Good	Normal pattern	Interstitial markings	Nodule	Consolidation
Cortical margins	4.37 [0.67]*	4.29 [0.65]*	4.10 [0.71]*	4.15 [0.67]*	4.34 [0.61]*	4.40 [0.67]	4.12 [0.72]*	4.38 [0.61]*	4.32 [0.55]*
Trabeculae	3.47 [1.4]*	3.49 [1.39]*	3.67 [1.3]	3.35 [1.5]*	3.61 [1.29]*	3.60 [1.2]*	3.42 [1.5]*	3.48 [1.4]	3.57 [1.3]*
Left diaphragm	12.6 [3.7]*	11.5 [5.3]*	8.63 [6.6]	10.3 [5.8]	11.4 [5.3]*	13.9 [2.8]*	9.10 [6.1]	13.5 [3.2]*	10.6 [5.8]
Spine	9.27 [4.7]*	8.26 [5.0]*	6.23 [4.1]	6.92 [4.7]	8.68 [4.9]	8.87 [4.3]	6.67 [4.9]	7.71 [4.9]	9.24 [4.8]*
Trachea	11.9 [3.8]*	13.8 [3.1]*	13.8 [3.9]*	13.9 [2.6]*	13.4 [3.8]*	13.6 [3.5]*	14.4 [2.5]*	12.6 [3.9]*	13.5 [3.7]*
Diaphragm	14.2 [2.4]*	12.3 [5.0]*	9.33 [6.0]*	11.3 [5.7]	12.1 [5.1]*	14.7 [1.5]*	11.3 [5.4]	14.5 [2.0]*	10.1 [6.3]*
Pulmonary vasculature	23.4 [9.5]	20.5 [11]*	19.1 [12]*	19.3 [12]	21.2 [11]*	27.1 [5.0]*	15.0 [12]*	27.4 [5.9]*	19.0 [11]
Contrast	21.1 [8.8]*	20.0 [9.2]*	16.6 [7.5]	18.2 [8.7]	20.0 [9.6]*	25.8 [8.0]	18.1 [9.7]	20.8 [8.2]*	17.8 [8.8]*
Graininess	19.5 [1.8]*	19.5 [1.8]*	19.3 [2.1]*	19.3 [2.1]*	19.5 [1.8]*	19.5 [1.8]*	19.5 [1.8]*	19.1 [2.3]*	19.6 [1.6]*
Density	10.5 [2.4]*	10.2 [2.7]*	9.17 [2.3]	9.68 [2.6]	10.4 [2.6]*	11.7 [2.7]	9.25 [2.7]	10.5 [2.36]*	10.2 [2.3]*
Detail	19.0 [5.5]*	19.6 [4.8]*	17.7 [5.7]	18.5 [5.1]*	19.5 [4.8]*	21.3 [5.7]	18.0 [5.8]*	19.2 [4.5]*	19.6 [4.3]*
Total score	74.7 [11]*	71.7 [11]*	63.8 [12]*	67.4 [12]*	72.1 [11]*	82.3 [9.7]*	64.4 [13]*	76.6 [9.3]	68.8 [8.1]*

BMI, body mass index; CIP, conventional image processing; NIP, new image processing.

* $P < 0.05$: Comparison with the score of CIP.

the poor group scores were significantly higher than CIP. In the lung lesion category, the total score was higher in order of a normal pattern, a nodule, a consolidation and interstitial markings. The total score was significantly improved in comparison with CIP, except in the nodule group.

DISCUSSION

By calculating the NPS, we confirmed the effect of noise reduction by NRP. The NPS values with NRP were small for all spatial frequencies, which indicates that NRP can reduce image noise in various chest structures. The difference in density resolution between the 2 processing methods was confirmed by the C-D diagram. Figure 3 shows that the 72% of IQF with NIP (factor 5) was equal to 100% of IQF with CIP. Therefore, it is possible to reduce the radiation dose when using the NRP.

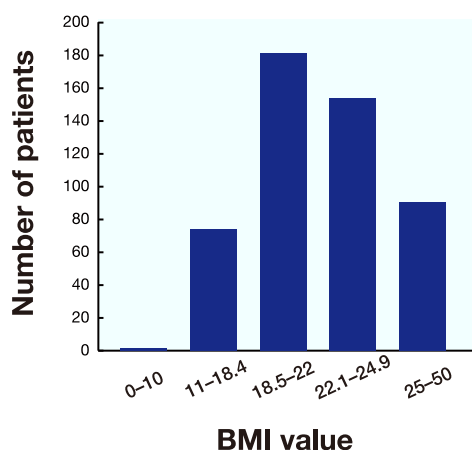


Fig. 4. The distribution of BMI over 1 week in patients examined by chest radiography. Many patients had a BMI above the normal range. BMI, body mass index.

The score for NIP (factor 7) was significantly higher than CIP in the phantom study; however, the score for NIP (factor 5) was the opposite in the clinical study. The chest phantom image is unvaried compared with the clinical image. Thus, observer performance likely improved because the evaluation became easier, i.e., the decrease in image noise was enhanced by noise reduction, which facilitated evaluation. Some reports suggest that excessive image processing deteriorates X-ray image quality.^{7, 8} In this study, the moderate processing NIP (factor 5) was more useful than the strong processing NIP (factor 7). This result corresponded with the results of past reports. We were also able to confirm the usefulness of NIP (factor 5) in clinical cases with interstitial markings or high BMI. In cases of diffuse interstitial markings, the contrast and density of the lung are reduced, which inhibits recognition of the pulmonary vasculature and the minor fissure. Using NIP (factor 5), the discrimination in the lung field was improved by noise reduction and frequency emphasis, thus the score improved. There was a tendency for the overall score of the high BMI group to decrease; however, the score improved by 13% using NIP (factor 5). Figure 4 shows the distribution of BMI over 1 week in patients examined by chest radiography. Many patients had a BMI above the normal range. This led us to believe that there are many imaging situations where NRP can be effective.

In this study, strong image processing decreased the image noise in the physical characteristic analysis; however, moderate image processing was most suitable for the evaluation of clinical cases. Consequently, we were able to optimize the image processing for chest radiography by using NRP. These processes for optimization will likely benefit any radiography facility.

Acknowledgments: The authors wish to thank Mr. Akira Hagiwara of (Foundation) Kanagawa Prefectural Association of Preventive Medicine, Japan, for providing the reference of BRH method. We are also indebted to Mr. Yoshiharu Hirata of Division of Clinical Radiology, Tottori University Hospital, Japan, for helpful discussions and assistance to this study.

The authors declare no conflict of interest.

REFERENCES

- 1 Hosch WP, Fink C, Radeleff B, Kampschulte A, Kauffmann GW, Hansmann J. Radiation dose reduction in chest radiography using a flat-panel amorphous silicon detector. *Clin Radiol.* 2002;57:902-7. PMID: 12413914.
- 2 Ishida M, Paul H. Frank, Doi K, Lehr JL. High quality digital radiographic images: improved detection of low-contrast objects and preliminary clinical studies. *Radiographics.* 1983;3: 325-38.
- 3 Manninen H, Partanen K, Soimakallio S, Rytönen H. Image-intensifier photofluorography and conventional chest radiography: comparison of diagnostic efficacy. *AJR Am J Roentgenol.* 1988;150:329-44. PMID: 3257605.
- 4 Kheddache S, Manson LG, Angelhed JE, Denbratt L, Gottfridsson B, Schlossman D. Effects of optimization and image processing in digital chest radiography: an ROC study with an anthropomorphic phantom. *Eur J Radiol.* 1991;13:143-50.
- 5 Chotas HG, Ravin CE. Digital chest radiography with a solid-state flat-panel X-ray detector: contrast-detail evaluation with processed images printed on film hard copy. *Radiology.* 2001;218:679-82. PMID: 11230639.
- 6 Bacher K, Smeets P, Bonnarens K, De Hauwere A, Verstraete K, Thierens H. Dose reduction in patients undergoing chest imaging: digital amorphous silicon flat-panel detector radiography versus conventional film-screen radiography and phosphor-based computed radiography. *AJR Am J Roentgenol.* 2003;181:923-9. PMID: 14500203.
- 7 Niklason LT, Chan HP, Cascade PN, Chang CL, Chee PW, Mathews JF. Portable chest imaging: comparison of storage phosphor digital, asymmetric screen-film, and conventional screen-film systems. *Radiology.* 1993;186:387-93. PMID: 8421740.
- 8 Kheddache S, Denbratt L, Erik J. Angelhed. Digital chest radiography—optimizing image processing parameters for the visibility of chest lesions and anatomy. *Eur J Radiol.* 1996; 22: 241-5.
- 9 Thijssen MAO, Bijkerk KR. Manual contrast-detail phantom artinis CDMAM Type 3.4. Nijmegen: University Medical Center St Radboud; 2006.
- 10 Cameron JR, Alter AJ. Optimization of chest radiography: proceedings of a symposium held at the University of Wisconsin, Madison, Wisconsin, April 30-May 2, 1979. Rockville: U.S. Dept. of Health and Human Services, Public Health Service, Food and Drug Administration, Bureau of Radiological Health; 1980. p. 237-48.
- 11 World Health Organization. Obesity: preventing and managing the global epidemic. Report of a WHO Consultation. WHO Technical Report Series. 2000;894:5-37.
- 12 Chida K. [The interpretation for chest X-ray radiography]. Tokyo: Nankodo; 2009. p. 38-148. Japanese.
- 13 Goodman LR. Felson's principles of chest roentgenology: a programmed text. 3rd ed. Philadelphia: Saunders; 2007. p. 52-3.